## Title

The ALS OSMS: Optical Surface Measuring System for high accuracy two-dimensional slope metrology with state-of-the-art x-ray mirrors



## ISBN

9781510620919

## Authors

Lacey, Ian
Anderson, Kevan
Centers, Gary P
et al.

## Publication Date

2018

## DOI

10.1117/12.2321347

Peer reviewed

# The ALS OSMS – Optical Surface Measuring System for high accuracy two-dimensional slope metrology with state-of-the-art x-ray mirrors

Ian Lacey,[*a] Kevan Anderson,[a] Gary P. Centers,[a,b] Ralf D. Geckeler,[c] Gevork Gevorkyan,[a] John Grossiord,[d] Andreas Just,[c] Theo Nicolot,[d] Brian V. Smith,[a] and Valeriy V. Yashchuk[a]
[a]Lawrence Berkeley National Laboratory, 1 Cyclotron Rd., Berkeley, California 94720; [b]Helmholtz Institute, JGU Mainz, Staudingerweg 18, 55128 Mainz, Germany; [c] Physikalisch-Technische Bundesanstalt, Bundesallee 100, D-38116 Braunschweig, Germany; [d]Institut Universitaire de Technologie Le Creusot, 12 Rue de la Fonderie, 71200 Le Creusot, France

## ABSTRACT

To preserve the brightness and coherence of x-rays produced by diffraction-limited-storage-ring (DLSR) and free-electron-laser (FEL) light sources, beamline optics must have unprecedented quality. For example, in the case of the most advanced beamlines for the DLSR source under development at the Advanced Light Source (ALS), the ALS-U, we need highly curved x-ray mirrors with surface slope tolerances better than 50–100 nrad (root-mean-square, rms). At the ALS X-Ray Optics Lab (XROL), we are working on the development of a new Optical Surface Measuring System (OSMS) with the required measurement accuracy. The OSMS is capable for the two-dimensional (2D) surface slope metrology over the spatial range from the sub-mm scale to the clear aperture. Usage of different arrangements of the OSMS sensors allows measuring the mirrors in the face-up or side-facing orientation, corresponding to the beamline application. The OSMS translation system and data acquisition software are designed to support multi scan measurement runs optimized for automatic suppression and compensation of instrumental drifts and major angular and spatial systematic errors. Here, we discuss the recent results of the OSMS research and development project. We provide details of the OSMS design and describe results of experimental performance tests of the gantry system. In particular, we show that the system is capable for measurement repeatability with strongly curved mirrors on the level of 20 nrad (rms). The high angular resolution of the OSMS rotational tip-tilt stage is adequate for implementation of instrumental calibration with using the mirror under test as a reference. The achieved measuring accuracy is demonstrated via comparison to metrology with the carefully calibrated Developmental Long Trace Profiler, also available at the XROL.

**Keywords:** Synchrotron radiation, error suppression, wave-front preservation, calibration, metrology of x-ray optics, surface metrology, DLSR, FEL.

## 1. INTRODUCTION

To preserve the brightness and coherence of x-rays produced by diffraction-limited-storage-ring (DLSR) and free-electron-laser (FEL) light sources, beamline optics must have unprecedented quality. For example, in the case of the most advanced beamlines for the DLSR source under development at the Advanced Light Source (ALS), the ALS-U,[1,2] we need highly curved x-ray mirrors with surface quality characterized with residual (after subtraction of an ideal shape) surface slope and height errors of <50−100 nrad (root-mean-square, rms) and <1−2 nm (rms), respectively. The x-ray optics of the same quality as that of the DLSR sources are required to entirely exploit the advantages of the fourth-generation synchrotron light sources and fully coherent free electron lasers (FELs).[3-7] The ex-situ metrology that supports the optimal usage of these optics at the beamlines must offer even higher measurement accuracy (see, for example, Ref.[8] and references therein). Specifically, for the ALS-U project, we need reliable and efficient surface metrology tools with a reasonably high measurement rate suitable for metrology with a large amount of optics coming for characterization, assembly, tuning, and alignment in the rather short period of time scheduled for installation of all the optics at ALS-U beamlines.

At the ALS, the ex-situ metrology is concentrated in the X-ray Optics Metrology Laboratory (XROL).[9,10] The XROL is in operation in a dedicated laboratory space with comprehensive control of environmental conditions. This is a cleanroom facility a factor of ~5 better than class 1000, with temperature stability better than ±30 mK over a day.[9,10]

* ILacey@lbl.gov; phone 1 510 495-2159; fax 1 510 486-7696

The superior environmental conditions are vital for operation of all metrology instrumentation in the lab with the high measurement repeatability. Currently, the lab equipment includes, in particular, two slope-measuring long-trace profilers, upgraded LTP-II[11,12] and DLTP.[13,14] With these instruments, the XROL delivers the state-of-the-art surface slope metrology required to build and maintain high performance operations of the ALS beamlines.[15] For example, the upgraded LTP-II and DLTP are capable of one-dimensional surface slope profiling with the proven accuracy of tangential slope measurements with flat optics of ~60 nrad (rms) and accuracy with significantly curved optics (radius of curvature of 15-20 m) of ~200 nrad limited by the profiler's systematic errors.

The current performance of the slope profilometry at the ALS XROL is close to the requirements for the ALS-U optics only for measurements with plane and relatively small optics. The accuracy achieved in measurements with significantly curved and sagittally shaped optics is worse by a factor of about 2-4. This reflects the general situation with ex situ metrology for x-ray optics. The increasing requirements for optical elements have led to significant ongoing efforts among the optics teams at almost all x-ray facilities around the world. The ex situ metrology challenges are shared, and we anticipate that hard work will result in new tools and continued advances over time. Here are several examples of advanced work and active collaborations underway.

In recent years, the work of Prof. Kazuto Yamauchi's laboratory at Osaka University (Japan), has led to the development of surface-polishing technology and dedicated metrology known as elastic emission machining (EEM),[16] micro-stitching interferometry (MSI),[17,18] and relative-angle determinable stitching interferometry (RADSI).[19,20] These technologies have been transferred to Japanese industry that now supplies unprecedented ultra-precision x-ray optics. Unfortunately, the RADSI and MSI systems are not currently available on the market.

At the ALBA Synchrotron Light Source (Spain), a radical improvement of the measurement rate of the nanometer optical component measuring machine (NOM) profiler based on electronic autocollimator (AC) and movable pentaprism, originally developed at the HZB/BESSY-II,[21,22] was made by implementing a continuous-scan ("on the fly") mode of operation.[23] A special procedure for data acquisition and analysis allows overcoming the problem of correspondence between mirror position and slope (specific for NOM systems based on the autocollimators without an electronic trigger). It was demonstrated that the average of multiple measurements taken with the ALBA-NOM using the on-the-fly mode provides surface slope data with ultimate low noise and high accuracy for measurement time reduced by a factor of approximately 4-5.[23]

The capability for fast scanning opens a new avenue for the application of the systematic error suppression method developed at the SOLEIL (France)[24] based on a large number of independent-redundant measurements of the surface under test (SUT) with changing the pitch alignment of the mirror between scans. With the regular slow mode of scanning, the method suffers from the temporal angular instability of the measurement set-up.

The reliability and efficiency of the calibration of a slope profiler can be significantly improved by using the SUT as a reference mirror when calibrating the profiler, avoiding the need for a universal multi-dimensional calibration, accounting for all possible shapes of SUTs and measurement arrangements. A low-budget tilting stage capable for accommodation large x-ray mirror substrates is in use at the HZB/BESSY-II optics lab.[25] It can be thought of as a prototype of the stage for direct calibration with the SUT. However, the stage for this application must provide pitch tilting with a pivot axis on the SUT optical surface; such is not the case for the stage in the HZB/BESSY-II optics lab.

A stitching Shack-Hartmann optical head (SSH-OH) for 2D surface-slope profilometry was developed at NSLS-II (Brookhaven) in collaboration with Imagine Optic (France).[26] A commercially available version of such a profiler with brand name SHARPeR has been developed through a collaboration between Image Optic and Q-Sys [27] The capability of SHARPeR for high accuracy measurements with strongly curved x-ray mirrors still has to be demonstrated.

One more prospective sensor for an advanced slope profiler is that of an LTP-type multi-beam optical sensor, under development in collaboration between the metrology teams at the ALS and NASA Marshall Space Flight Center (MSFC) (see Ref.[28] and references therein). Similar to the Shack-Hartmann sensor, the multi-beam sensor is capable of 2D measurement with stitching, realizing an idea of differential measurements, significantly free of the measurement errors associated with the carriage wobbling and temporal drift.

LTP-like deflectometers, when equipped with a single-mode wavelength-stabilized laser light source, are capable of high-precision measurements of the groove density distribution of varied line spacing (VLS) x-ray diffraction gratings having groove densities from ~60 lines/mm and up to approximately 2,800 lines/mm.[29-31] Note that the grating groove density measurements with a NOM-like profiler using an AC with a LED light source are impossible.

The listed developments constitute just a few examples of the diverse and heroic efforts of the x-ray optics metrology community directed towards integration of all of the basic schematics and principles placed in the foundation of current instruments into a single, universally applicable, x-ray metrology instrument. Unfortunately, no such universal solution for an instrument capable of state-of-the-art performance for all x-ray metrology tasks has been found. Nevertheless, some progress on this still should be possible, given significant innovation, and would be very welcome, considering the perennial limited nature of funding for x-ray metrology.

At the ALS X-Ray Optics Lab (XROL), we are working on the development of a new Optical Surface Measuring System (OSMS) with the desired accuracy beyond 50 nrad (absolute).[32,33] Our OSMS project is, in some sense, a continuation of the efforts of a broad collaboration including DOE x-ray facilities and vendors of x-ray optics with active participation of the HBZ/BESSY-II optics group[34] that formulated the major requirements to the design and performances of the OSMS gantry system. Based on the consideration in Ref.,[34] a high-performance gantry system for a new generation of optical slope measuring profilers has been developed for the Argonne Photon Source (APS).[35,36] Similarly to many other laboratories (see, for example, Refs.[23,26,37,38]), we have adopted the design of the gantry system firstly developed for the HZB/BESSY-II NOM.[21,22]

The NOM-like gantry system of the OSMS at the ALS XROL is capable for the two-dimensional (2D) surface slope metrology over the spatial range from the sub-mm scale to the clear aperture. The distinguished feature of our gantry system is the custom combined rotary and alignment stage (tip, tilt, pitch, and rotation, TTPR, stage). The gantry system and the original data acquisition software are designed to support multi-scan measurement runs optimized for automatic suppression and compensation of instrumental drifts and major angular and spatial systematic errors[33,39,40] with different types and arrangements of sensors.

In this paper, we discuss the recent results of the OSMS research and development project. We start (Sec. 2) from a brief consideration of the major limited factors in the slope profilometry and the experimental methods for overcoming the limitations. Based on this consideration, in Sec. 3 we review the groundwork conceptions and design features of the ALS XROL OSMS. In particular, we discuss performance of the OSMS in different arrangements of four autocollimators used as surface slope sensors. Different combinations of the sensors are used for measuring the mirrors in the face-up or side-facing orientation matched to the beamline application. In Sec. 4, we formulate the performance requirements to the rotation and translation system. Sections 5 and 6 describe results of experimental performance tests of the carriage and slab translations in the spatial and angular domains. In Sec. 7, we investigate the performance of the OSMS TTPR and show that the high angular resolution of the TTPR stage is adequate for implementation of instrumental calibration with using the SUT as a reference. We demonstrate that the system is capable for measurement repeatability with strongly curved mirrors on the level of 20 nrad (rms). In Sec. 5, the achieved measuring accuracy is demonstrated via comparison to metrology with the carefully calibrated DLTP, also available at the XROL.

## 2. DATA ACQUISITION METHODS FOR SUPPRESSION OF INSTRUMENTAL DRIFT AND SYSTEMATIC ERRORS

The achieved high accuracy in slope measurements with the XROL LTP-II and DLTP has become possible due to the extremely high precision (repeatability) of the measurements, of < 40 nrad (rms), and by the application of sophisticated experimental methods developed at the XROL for suppression of the measurement errors due to random noise, drift, and instrument systematic errors. [33,39,40] Because any new profiler should be capable for implementation of these and other methods developed and used at the XROL for high precision surface slope measurements, we briefly describe them below in this section.

Besides the advanced environmental conditions in the lab, the high repeatability of the measurements is achieved with the 'move-stop-wait-measure-…' mode of data acquisition with the profilometer. In this case, we exclude the error due to the random wobbling and wiggling of the profiler's cartridges. The price to pay is the very slow measurement rate with the one-point acquisition time of about 12 sec for the LTP-II and about 3 sec for the DLTP.

In order to suppress the measurement error associated with the profiler's temporal drift (including pointing instability of the LTP-II laser beam), we have developed and routinely apply an original experimental method[39] that we call optimal scanning strategy (OSS) method. According to the method, each measurement is an average of surface slope traces recorded in an optimally arranged set of sequential scans with the profiler in the forward (F) and backward (B) directions. For example, the scanning strategy F-B-B-F-B-F-F-B for a measurement run of 8 sequential scans is optimal for suppression of the contribution to the error of polynomial drifts up to the third order.[39] Additionally, the averaging

efficiently suppresses the low frequency random noise due to air turbulence (see, for example, Ref.[41] and discussion in Sec. 6.1). A single run of 8 optimally arranged scans is usually enough to solve the problems of the drift error and significantly suppress the random noise. In Ref.,[33] the OSS method, originally developed for 1D slope profilometry, has been extended to two-dimensional measurements.

One of the solutions to the systematic error problem is the precision angular calibration of the profilers.[42,43] This helps only to some extent because of the strong dependence of the profiler's systematic error on the peculiarities of the measurements including the shape of the SUT.[44] Practically in slope measurements with significantly curved optics, the absolute accuracy achievable with the calibration with a flat reference is limited by approximately 200 nrad.

Better accuracy is achieved by applying correlation analysis to surface metrology data.[40] The method consists in randomization of the systematic error by the averaging of multiple measurements, specially arranged to make the systematic errors of the measurements to mutually anti-correlate by measuring at different tilts and translations of the SUT. Compared to the straightforward calibration of the profiler's systematic error with a reference mirror, the correlation method operates only with the measurements obtained with the SUT itself and, therefore, automatically accounts for the peculiarities of the measurements. In the case of a periodic systematic error, the optimal anti-correlated measurements are two measurements shifted by a half of the error period. With 180-degree flipping of the SUT, the even part of the systematic errors.[33]

The drawback of the methods discussed for suppression of the slope profiler's errors is a significant increase of the total measurement time necessary for measuring a single surface slope trace. For example, an optimal run of 8 scans over 400 mm clear aperture with 1-mm increment takes almost 11 hours when measuring with the XROL LTP-II and about 3 hours with the DLTP. When additional tests are required to anti-correlate the instrumental systematic error, total measurement time can reach a few days at non-stop running (including overnight runs).

Advanced optimal scanning strategies (AOSS)[33] have been recently developed at the XROL to improve the measurement time with a profiler equipped with a dedicated automated rotation and flipping stage.[45] The AOSS technique allows incorporating, in one measurement run of surface slope metrology, the advantages of the described methods for suppression of the random noise, drift and systematic errors, originally applied to a number of sequential runs. It provides a prescription for alteration within a single run of the SUT orientation (by flipping) and alignment (by tilting) additionally to the reversal of the scanning direction prescribed by the OSS method. Thus, in a single eight-scan run arranged according to the AOSS prescription, we get a significant, by a factor of about four, increase of the measurement rate at no degradation of the accuracy of the surface slope metrology.[33] A possibility for implementation of the AOSS technique in a new profiler is crucial.

## 3. THE ALS XROL OPTICAL SURFACE MEASURING SYSTEM

As we have pointed out above, development of a new generation of optical surface slope measuring profilers suitable for metrology with state-of-the-art x-ray optics needed for the DLSRs and FELs, has been a hot topic of research-and-development efforts of metrology teams at practically all x-ray light facilities around the world. Thus in 2010, a collaboration, including all US DOE synchrotron labs, industrial vendors of x-ray optics, and with active participation of the HBZ-BESSY-II optics group, discussed the major concepts of a new slope measuring profiler – the optical slope measuring system. The major goals of two collaborative meetings at the ALS (March 26, 2010) and at the APS (May 6, 2010) were to solidify design approaches that allow meeting the need of slope measurement accuracy of < 50 nrad.[34] Later, the ideas discussed at the meetings were implemented in a number of slope profilometers that are now in operation at the APS,[35,36] NSLS-II,[46] and ALS.[32,33] In this section, we briefly overview the groundwork concepts and design of the OSMS under development at the ALS XROL.

### 3.1 OSMS groundwork concepts and design

Our OSMS project at the XROL is, in some sense, a continuation of the efforts of this collaboration. The key element of the OSMS is its gantry system that, in our case, is better to call 'multifunctional translation system (MFTS) – Fig. 1. The standard NOM-like gantry system[21,22] allows automatically controlled scanning of the sensor optical head across the SUT in two orthogonal directions. Scanning along the longitudinal X-direction by maximum 1.5 m is provided with translation of a carriage air-bearing-suspended on a long beam of a bridge-type translation stage. By moving a base slab with large air-bearing surface across the base of the gantry system, the SUT can be translated by maximum ±150 mm along the sagittal Y-direction.

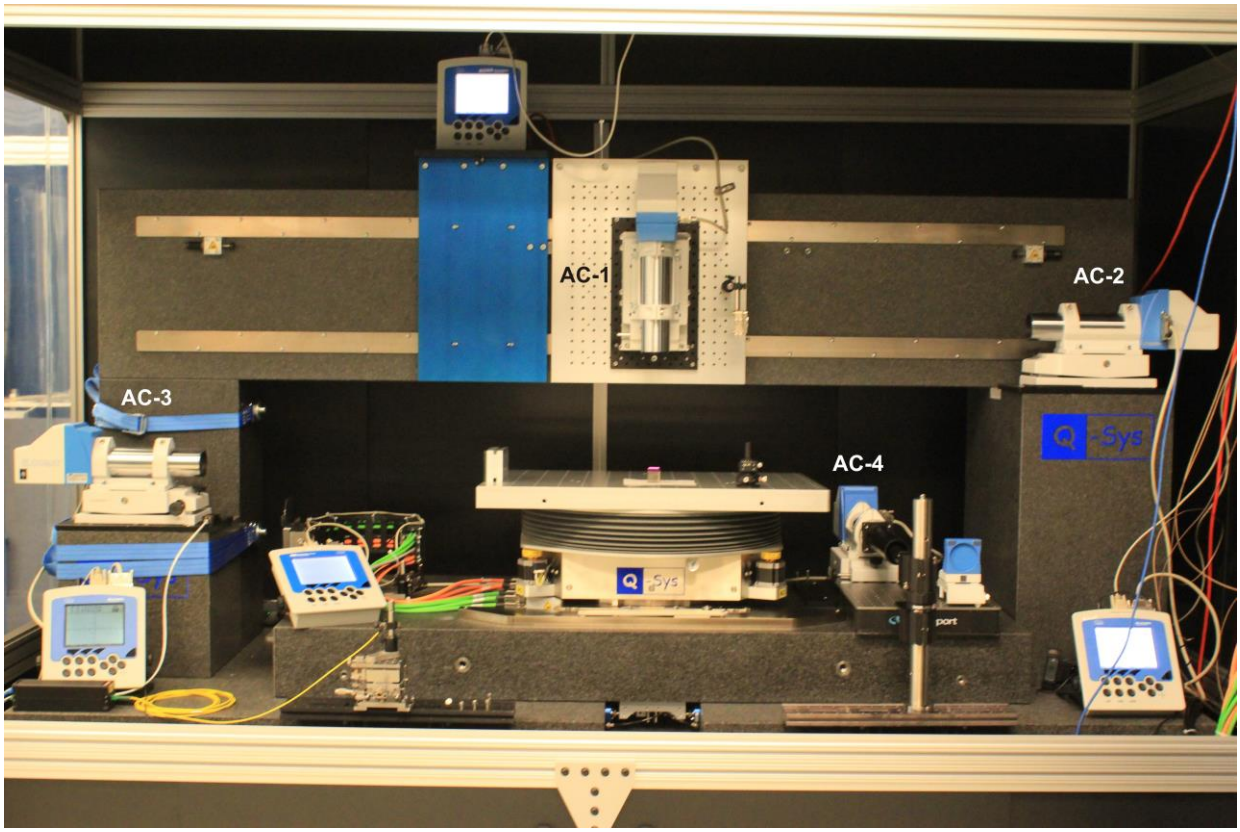


Figure 1: Experimental arrangement of the ALS XROL OSMS based on the multifunctional translation system (MFTS) and four electronic autocollimators ELCOMAT-3000.[54]

In addition to these two translations, the OSMS MFTS has a precise tip, tilt, pitch, and rotation stage capable for automatically controlled tilting and rotation (flipping) of the SUT in the course of a measurement run, as well as vertical (Z-axis) shifting of the SUT by maximum 50 mm. These additional translations are crucial for implementation of experimental methods,[33,39,40] discussed in Sec. 2, for automatic suppression of the errors in a measurement run via optimal arrangement of repeatable scans. The high angular resolution of the OSMS rotational tip-tilt stage is adequate for implementation of instrumental calibration with using the SUT as a reference (see Sec. 7).

The OSMS MFTS shown in Fig. 1 was custom designed and fabricated by Q-Sys Company.[47] All the motion controls and data acquisition systems are based on the NI LabView™ platform.

The OSMS setup is located in the ALS XROL clean-room. It is placed inside a two-layer enclosure consisting of a hutch and a plastic curtain system. Together with the advanced environmental conditions in the lab, the enclosure helps to additionally stabilize the temperature inside the hutch (Fig. 2) and, therefore, minimize the measurement errors due to the instrumental and SUT setup temporal drifts.

The temperature variation measured inside the OSMS hutch during an 8-hour long slope measurement run is depicted in Fig. 2 in the time and frequency (power spectral density, PSD) domains. There is a periodic oscillation with the period of ~4.8 min and the rms variation of about 2.4 mK. The temperature oscillation inside the hutch is due to the operation mode of the lab air-conditioning system.[9,10]

### 3.2 OSMS measurement arrangements

In the conventional NOM-like slope profilometer, a movable (preferably, mirror based[48,49]) pentaprism makes the measurements insensitive to the systematic error due to carriage wobble. The drawback of this schematic is the strong variation of the distance between the AC and the surface under test in the course of measurement. This makes difficult accounting of the AC systematic error by application of an angular calibration performed at the fixed distance.[50-53]

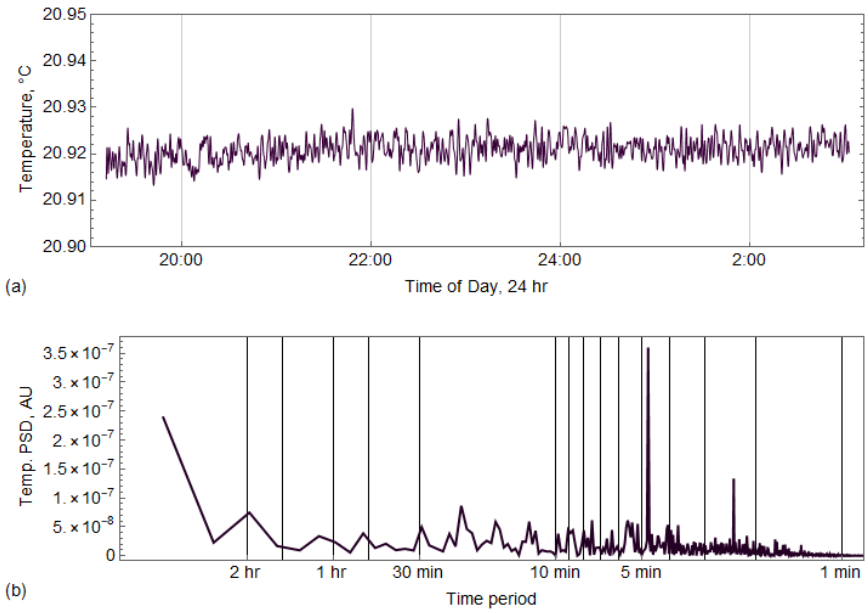


Figure 2: Temperature variation measured inside the OSMS hutch measured during a 5-hour long slope measurement run. The periodic oscillation with the period of ~4.8 min and the rms variation of about 5 mK is due to the operation mode of the lab air-conditioning system.[9,10]

Moreover, in the NOM-like arrangement the measurements are significantly affected by the air convection noise[41] due to the increased optical path through the air of the sensor's light beam incident to and reflected from the SUT.

Figure 1 shows the XROL OSMS measurement arrangements with one of four ELCOMAT-3000[54] autocollimators, AC-1, placed vertically on the OSMS translation carriage.[32,33] In the course of measurements, when the carriage with the AC is translated along the SUT, the distance between the AC and the SUT is practically unchanged. This allows a reliable application of the AC calibration performed at the same AC-to-SUT distance. Additionally, the problem of air convection noise in the SUT measuring (sample) channel is also solved with the aperture mounted to the AC with a close tube that shields the AC light beam optical path. The payment for these advantages is a necessity to control the wobbling error with an additional AC mounted on the right-hand granite stand, AC-2 in Fig. 1. Thus, the air convection noise problem is transferred to the reference channel. In Sec. 6.1, we show how we overcome the noise problem in this case.

To the best of our knowledge, the arrangement of an AC-based surface slope profilometer with a movable, vertically oriented AC and an additional AC in the reference channel was firstly considered in Ref.[55] and implemented and published in Ref.[46]

In the current arrangement of the XROL OSMS in Fig. 1, there are two more ACs that enable direct (without additional 90-degree folding mirror or pentaprism) measurements with side-facing oriented mirrors. The AC mounted on the left-hand granite stand, AC-3 in Fig.1, serves as a constant-distance measuring sensor; whereas the AC mounted to the movable slab, AC-4, is used in the reference channel monitoring the yaw-angle translation error of the slab.

### 3.3 2D slope measurements with the XROL OSMS

In Ref.[56], in order to get a 2D slope topography of the SUT, multiple 1D tangential traces are measured with a sequential translation of the SUT in the sagittal direction. In order to account for the drift error and misalignment of the mirror upon the sagittal shifts, additional sagittal and diagonal traces are used to reliably stitch the tangential traces. This significantly complicates and draws out the 2D data acquisition and data processing.

With the AC-1 in the sample channel and the AC-2 and AC-4 in two additional reference channels, we solve the problem of the wobbling error of the carriage and slab translations in our OSMS profiler.

The drift error in the 2D measurements is solved by application of the optimal scanning strategy method[39] as suggested in Ref.[33] and firstly realized in Ref.[34]

The idea of the extension of the OSS method to the 2D profilometry is illustrated in Fig. 3. Figure 3 shows the 2D scanning traces in the 'forward' (Fig. 2a) and in the 'backward' directions. The 2D traces in Fig. 2 can be mentally starched to the corresponding longer 1D traces scanned in opposite direction. Therefore, in 2D case it is also applicable the consideration of drift suppression with OSS methods suggested and mathematically proved in Ref.[39]

Similar to the 1D case[39] (see also Sec. 2), the scanning strategy F-B-B-F-B-F-F-B for a 2D measurement run of 8 sequential 2D scans arranged according to Fig. 3 is optimal for suppression of the contribution to the error of polynomial drifts up to the third order. Besides the automatic suppressing the drift error, the averaging of the 2D scans of an optimally arranged run efficiently suppresses the low frequency random noise due to air turbulence.

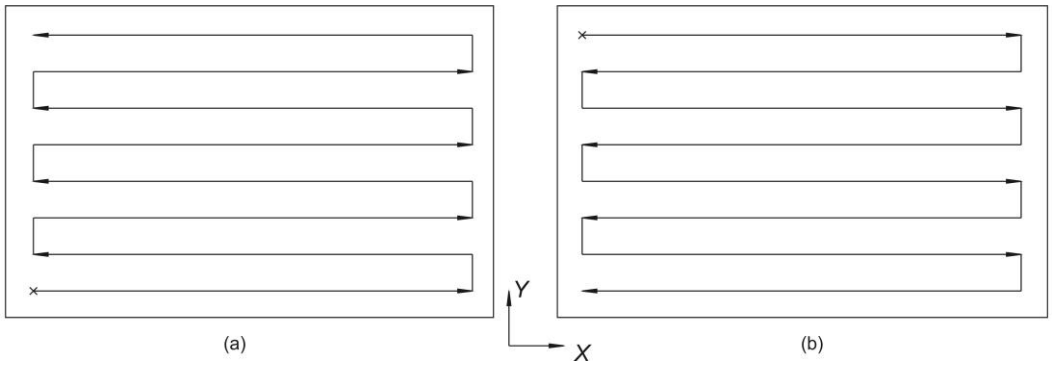


Figure 3: (a) 2D scan in the forward and (b) in the backward direction.[33] The 2D scans starting from tracing in *X*-direction are shown. A similar definition of the forward and backward scans can be applied to 2D scans that start from the measurement in *Y*-direction. The crosses depict the starting points of the scans.

### 3.4 Calibration of the OSMS autocollimators

The autocollimators in usage with the XROL OSMS have been precisely calibrated at the Physikalisch-Technische Bundesanstalt (PTB), Germany using their sophisticated experimental method and set-up.[57-59] With a highly stable AC, angular calibration with standard uncertainty down to about 15 nrad is possible.[50-53] Unfortunately, due to technical reasons, the calibration at the PTB cannot be performed at the AC-reference mirror distance of 80-85 mm, corresponding to the experimental arrangement of the OSMS AC-1 (Fig. 1). The required calibration was performed at the ALS XROL using a high precision tilt stage[43] developed as a key element to universal test mirror for characterization and calibration of slope measuring instruments.[42]

Recently, one of our ACs was calibrated at the PTB when equipped with a number of circular and rectangular apertures placed at different distances from the AC.[60] It was shown that reliable surface slope measurements with the profilometer using ELCOMAT-3000 autocollimator can be performed with a rectangular aperture with the tangential width as small as 1.5 mm (at the sagittal width of 3 mm). Usage of rectangular apertures in the AC-based slope profilometers opens a unique opportunity for reliable combining the measurements performed with low and high resolution (with large and small tangential width of the aperture, respectively).[60]

Figure 4a presents a characteristic example of the angular calibrations of one of the OSMS ACs equipped with different beam-collimating apertures: 2.5 mm and 1.5 mm diameter circular apertures and 1.5 mm × 3 mm rectangular aperture. There is a strong quasi-periodic variation in all calibration curves with angular period of about 310 μrad that is clearly seen in the power spectral density distribution of the calibration curves – Fig. 4b. This quasi-periodic systematic error is very characteristic for ELCOMAT-3000 ACs. In order to suppress the systematic error, we performed two sets of measurements performed at the pitch angles different by a half of the period.

When the oscillation periods of the AC calibration are very stable, the absolute calibration strongly depends on the peculiarities of the measurement set-up (for example, the aperture alignment, shape and size, distances from the SUT to the AC and aperture, etc.), as well as on the shape and size of the SUT. A radical solution to the problem of the absolute calibration is to carry out the calibration in the particular measurement arrangement using the SUT as a reference mirror. We call it as the self-calibration method. For implementation of this method, one needs a high resolution tilting stage that is capable for pitch tilt of the SUT with the rotation axis positioned on the mirror surface area used for the calibration. In Sec. 7, we provide the results of the tests with the OSMS TTPR stage that suggest for the performance of the stage rotation and tilting adequate for the self-calibration.

Measurements of the lateral resolution, or more generally, the optical transfer function (OTF), of the AC equipped with1.5 mm × 3 mm rectangular aperture were performed at the ALS XROL.[60] For the OTF measurements, an original chirped-like test surface[61] developed by the collaboration of the HZB/BESSY-II and ALS metrology team and fabricated at the Leibnitz Institut für Oberflächen Modifizierung (IOM) in Leipzig[61,62] was used. The used chirped profile sample is designed to have a constant (independent on spatial frequency) amplitude in the slope domain.[62] Such sample provides highly confident information of the profilometer's resolution. It was demonstrated that the AC with the rectangular aperture has significantly higher spatial resolution in the tangential direction compared to the conventional 2.5-mm diameter circular aperture.

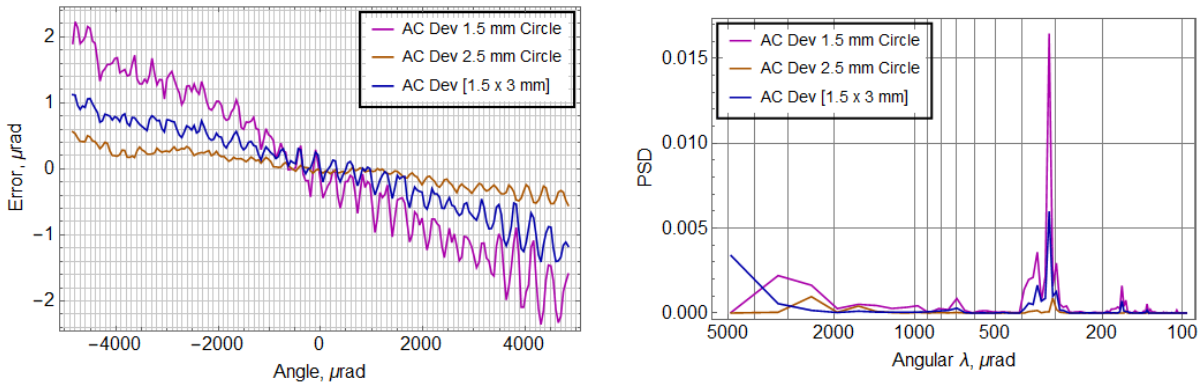


Figure 4: (a) ELCOMAT-3000 autocollimator calibrations with circular apertures of 2.5 mm and 1.5 mm diameter and 1.5 mm × 3 mm rectangular aperture. (b) The power spectral density distributions of the corresponding calibration traces. The calibrated tangential angular range is ± 4848 μrad. The distance between the AC and the collimating aperture is about 330 mm. The calibration was performed at the PTB, Germany.

## 4. PERFORMANCE REQUIREMENTS TO THE OSMS MULTIFUNCTIONAL TRANSLATION SYSTEM

The requirements to the performance of a multifunctional translation system for a surface slope profilers designed for high accuracy metrology with state-of-the-art x-ray mirrors were formulated, for example, in Refs.[34,45]

Here, in order to estimate the requirements for the current needs for metrology accuracy, we assume that the overall absolute error of the measurements must be less than 50 nrad. Correspondingly, we require the absolute errors related to the uncertainty of the sample beam positioning and the SUT mis-alignment due to the imperfection of flipping of its orientation to not surpass $\delta\beta = 10$ nrad.

First, we consider a highly curved tangential cylindrical mirror with an extreme radius of curvature equal to 15 m. In order to ensure the measurement error due to the uncertainty of sample beam positioning $\delta\beta$ better than ±10 nrad, the OSMS MFTS must be capable for spatial translation along the SUT with the absolute accuracy $\delta x$ better than ± 0.15 μm.

In order to estimate the accuracy of flipping an SUT, we consider two practical cases.[43] These are the flipping of the tangentially curved cylindrical mirror with the radius of curvature of 15 m (Fig. 5a) and a sagittally curved cylindrical mirror with sagittal radius of curvature of 30 mm (Fig. 4b). The geometrical parameters of the optics are chosen based on ALS-related applications.

Following to Ref.[45] for the case in Fig., 5a, the accuracy $\delta\alpha$ of 180-degree flipping has to be (assuming $R >> L$)

$$\delta\alpha \le \delta\beta^{1/2}\left(R/L\right)^{1/2}. \tag{1}$$

Substituting to Eq. (1) $R = 15$ m and $2L = 300$ mm, we get rather week tolerance to the accuracy of flipping of the tangentially curved cylindrical mirror:

$$\delta\alpha \le 1\,\text{mrad}. \tag{2}$$

For a sagittaly curved mirror (Fig. 5b) with $R = 30$ mm and $2L = 600$ mm, the required accuracy of flipping can also be estimated with Eq. (1). In this case, the flipping error has to be

$$\delta\alpha \leq 30 \text{ μrad.} \tag{3}$$

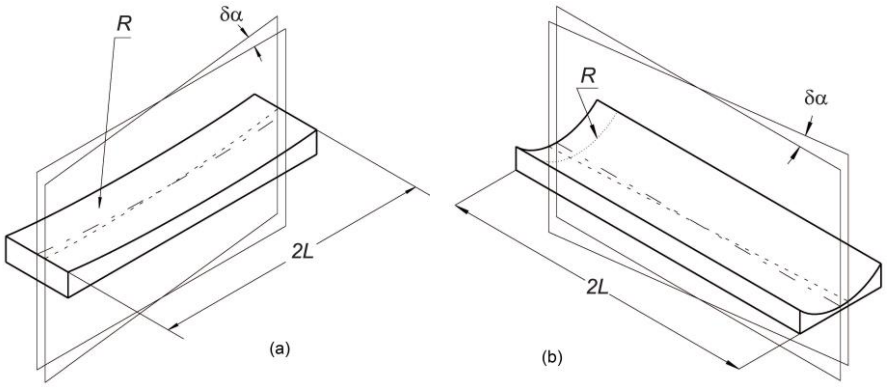


Figure 5: (a) Sketch of a surface slope measurement with a tangential cylinder with the radius of curvature $R$ and the length of $2L$. A misalignment between the measured trace (a dashed line) and the cylinder's section line (shown with a dot-dashed line) is denoted by $\delta\alpha$. The misalignment leads to a spurious systematic decrease of the surface slope along the measured trace compared to the measurement along the section line. (b) Sketch of a surface slope measurement with a sagittal cylinder with the radius of curvature of $R$ and the length of $2L$. A misalignment between the measured trace (a dashed line) and the cylinder's generating line (shown with a dot-dashed line) is denoted by $\delta\alpha$. The misalignment leads to a spurious variation of the surface slope along the measured trace.

Below, we present the results of investigation of performance of the OSMS multifunctional translation stage and compare them with the estimated requirements.

## 5. PERFORMANCE OF THE MFTS SPATIAL TRANSLATIONS

The performance of linear translations of the OSMS MFTS carriage and granite slab has been investigated in Ref.[32] In this work, the displacement measured with the corresponding MFTS built-in linear encoders was compared with the distance measured with the additional reference interferometers. As the references, an OPTODYNE displacement measuring interferometer (DMI)[63] and an Attocube integrated displacement sensing (IDS) interferometer[64] were used. Usage of two different reference interferometers allowed separation of the errors related to the translation stage from the systematic errors in the reference measurements.

Below, we briefly summarize the results in Ref.[32]

### 5.1 *X*-axis translation with the carriage

Tests of *X*-axis translation of the OSMS carriage by 1 meter have brought out a nonlinear error of the carriage positioning with the built-in linear encoder with the peak-to-value (PV) variation of ± 1 μm. The linear calibration factor of the encoder is equal to one with accuracy of about $5\times10^{-6}$. The nonlinear error has a strong systematic character with repeatability on the level of the resolution of the measurements with the OPTODYNE DMI of approximately 0.2 μm. Therefore, after precision measurement, the error carriage positioning can be accounted in the measurement control and data processing software.

For measurements with relatively short optics, with the length smaller than ~300 mm, we can use *X*-scanning within the carriage translation interval with the nonlinear error reduced to approximately ± 0.2 μm. This is close to the extreme requirement to the linear translation derived above.

### 5.2 *Y*-axis translation with the granite slab

In the case of the granite slab translation by the entire range of ±150 mm, the linear calibration factor of the corresponding linear encoder built in the MFTS is equal to one with accuracy of better than $10^{-5}$. A nonlinear error of the slab positioning of about ±1 μm (PV) with a relatively sharp perturbation of about 0.6 μm (PV) was observed at the position of the index between approximately –8 mm and 8 mm. Additional tests have confirmed that this sharp

perturbation belongs to the *Y*-coordinate gantry positioning system. The measured *Y*-axis translation error is also repeatable on the level of 0.2 μm.

### 5.3 *Z*-axis translation with the TTPR stage

The TTPR stage can go up and down using the coordinated motion of the three motors, each having its own linear encoder used also to control the stage tilt. The total range of the *Z*-axis translation is about 50 mm. It was observed a periodical *Z*-positioning error with approximately 5 mm period. Tests with the DMI have shown that the amplitude of the error depends on the position of the retroreflector on the TTPR stage platform. The tests have also shown that the oscillations are due to oscillatory behavior of each motor-encoder system with the amplitude of about 2-3 μm (P/V); what is more, the oscillation are asynchronous. At the center of the platform, the *Z*-positioning error also appears but with smaller magnitude of ±0.5 μm.

The major result of the measurements is that the *Z*-axis translation is very linear and repeatable on the level of a micron. However, the measurements reveal a significant linear calibration error of about 3.9% that has to be accounted in the motion control software.

## 6. ANGULAR ERRORS OF THE MFTS SPATIAL TRANSLATIONS

The wobbling (the pitch angular error) and wiggling (the yaw angular error) of the linear translations of the carriage and granite slab have been investigated in the corresponding arrangements depicted in Fig. 1. In the tests, the translation ranges were 1000 mm and 300 mm for the carriage (*X*-direction) and the slab (*Y*-direction), respectively.

For the carriage translation, the pitch and yaw angles are measured with the autocollimator AC-2 and a reference mirror mounted to the carriage platform (Fig. 1). The angular performance of the slab translation is monitored with the autocollimator AC-4, placed on the top of the slab and a reference mirror attached to the OSMS MFTS base. Prior the measurements, the ACs and their reference mirrors were carefully mutually aligned with the goal to minimize the AC beam walk across the reference mirror in the course of translation. That is to minimize the error associated with the reference mirror surface imperfection. Additionally, the roll angle of each AC was aligned with respect to the corresponding translation plane in order to avoid (suppress) the cross-talk between the AC's *X*- and *Y*-channels when measuring in the course of translation the wobbling and wiggling of the carriage and slab.

### 6.1 Filtering out of the air convection error

The relatively short *Y*-direction scanning range allows shielding of the AC-4 beam optical path with a system of concentric tubes. This dramatically decreases the random, low frequency error due to air convection.[41] Unfortunately, such shielding is difficult (if not impossible) for the much longer optical path of the AC-4 beam. In this case, we implement numerical filtering of the air convection noise from the measured pitch and yaw variation traces. The proper size of the filter is selected based on the stability tests with and without shielding, performed in the course of the gantry performance measurements using the AC-4 and the slab reference mirror.

Figures 6 and 7 present the residual (after linear detrending) pitch slope variation recorded in AC-4 *Y*-channel as the functions of the slab position (*Y* translation coordinate) and the corresponding PSD spectra measured in a test of the AC-4 reference channel without and with the shielding around the optical path, respectively.

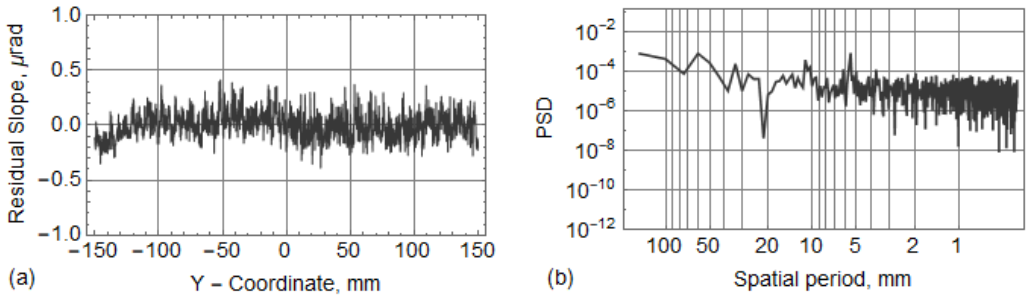


Figure 6: Without optical path shielding, (a) the residual (after subtraction of the best-fit linear dependence equivalent to 35.7 km of curvature) pitch slope variation and (b) the corresponding PSD spectrum as measured in the slab reference channel in AC-4 *Y*-channel. The rms variation of the residual slope trace in the plot (a) is 0.124 μrad.

The almost white noise like PSD spectrum in Fig. 6 is characteristic of air convection noise.[41] There is also a noticeable oscillation peak at spatial period 5.5 mm that corresponds to a temporal period of approximately 140 seconds. This is a harmonic of a known temperature oscillation of 280 seconds in the XROL due to the operation of the lab air conditioning system.

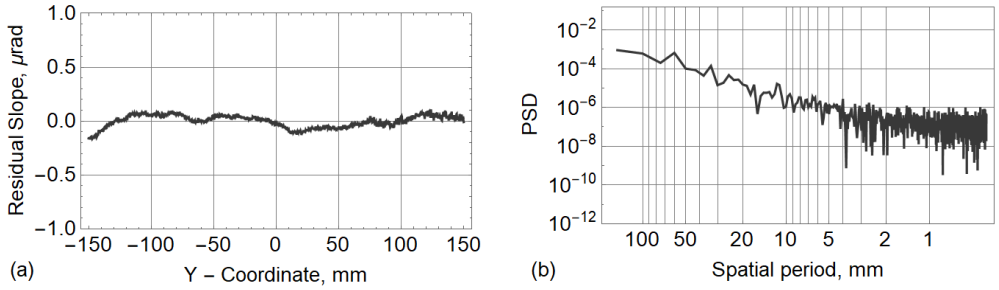


Figure 7: With optical path shielding, (a) the residual (after subtraction of the best-fit linear dependence equivalent to 36.9 km of curvature) pitch slope variation and (b) the corresponding PSD spectrum as measured in the slab reference channel in AC-4 *Y*-channel. The rms variation of the residual slope trace in the plot (a) is 0.057 μrad.

The AC-4 optical path shielding (Fig. 7) reduces the rms variation of the pitch angle temporal dependence by a factor of about 4. Correspondingly, the white noise like part of the PSD spectrum has decreased by almost two orders of magnitude, to the level that is now determined by the AC random noise.

The idea behind selection of the proper filter to suppress the air convection noise contribution in the reference channel is as follows. We apply the Gaussian filter in Mathematica™ to the PSD spectrum measured without shielding. The optimal size of the filter corresponds to situation when the white noise like distribution is filtered out over the spatial wavelength range below approximately 3 mm. This range corresponds to the white noise like part of the PSD spectrum measured with the shielding (Fig. 7b).

Figure 8 illustrates the suggested filtering procedure with the Gaussian filter size of 6 points (equivalent to 1.2 mm with data recorded at 0.2 mm increments).

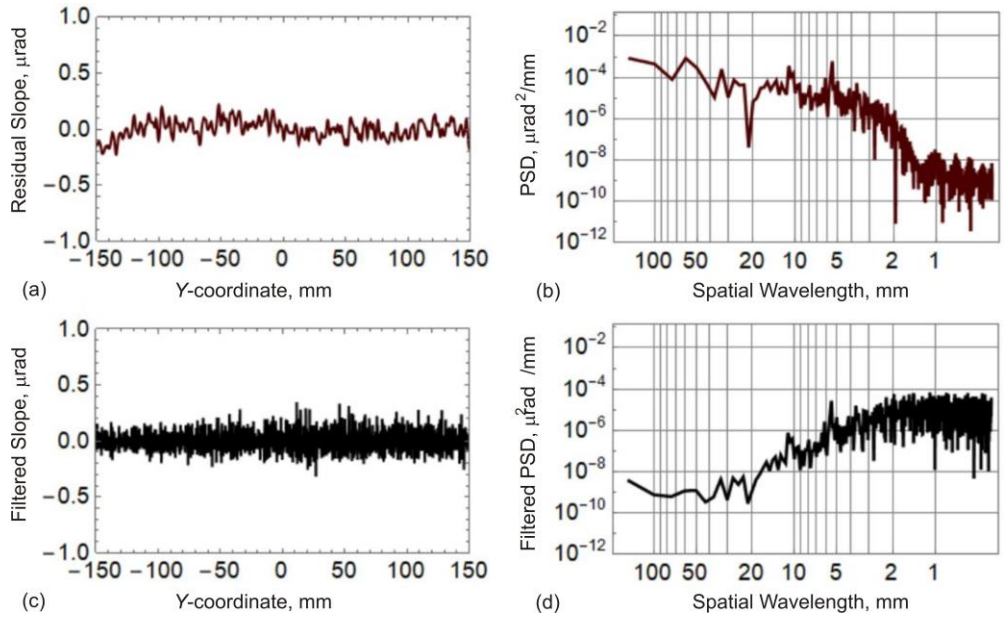


Figure 8: Without optical path shielding, (a) the residual pitch slope variation in Fig. 6a filtered with the Gaussian filter with size of 6 points (equivalent to 1.2 mm); (b) the PSD spectrum of the filtered trace in plot (a); (c) the filtered slope distribution equal to the difference between the unfiltered (Fig. 6a) and filtered [plot (a)] residual slope traces; (d) the PSD of the filtered out slope difference in plot (c). The rms variation of the filtered slope trace in the plot (c) is 0.089 μrad.

As desired, the filtered slope distribution in Fig. 8c that is equal to the difference between the unfiltered (Fig. 6a) and filtered (Fig. 8a) residual slope traces, has a white noise like spectrum at the spatial wavelengths smaller that approximately 3 mm. The rms variation of the filtered slope trace in the in Fig. 8c is 0.089 μrad. As an indication that the filter size is close to the optimum, the increase of the filter size to 12 mm the filtering only slightly change the rms variation of the filtered slope to the value of 0.098 μrad. Note that the applied filtering almost does not affect the 5.2-min oscillation peak.

Below, when discussing the wobbling and wiggling of the carriage translation along *X*-coordinate of the gantry system, the measured data are filtered with the filter selected here.

### 6.2 Angular errors of the carriage translations

The wobbling and wiggling effects of the carriage translation are illustrated in Figs. 9 and 10. The corresponding traces are the result of averaging of 8 scan used to suppress the measurement random and drift and errors (see Sec. 2). In order to suppress the random error due to the air convection, the slope traces in Figs. 9 and 10 have been filtered with the Gaussian filter discussed above, in Sec. 6.1.

The PV variation of the carriage pitch angle when scanning over 1000 mm (Fig. 8) is about 20 μrad. Most of the variation corresponds to the cylindrical shape (linear slope variation) that is due to the beam deformation upon gravity. The nonlinear residual slope variation is about 2.5 μrad (PV). Note that around the central part of the scanning range of ±100 mm, the wobbling error is almost perfectly linear, corresponding to the radius of curvature of ~50.3 km. This scanning range is preferable in metrology with relatively short optics.

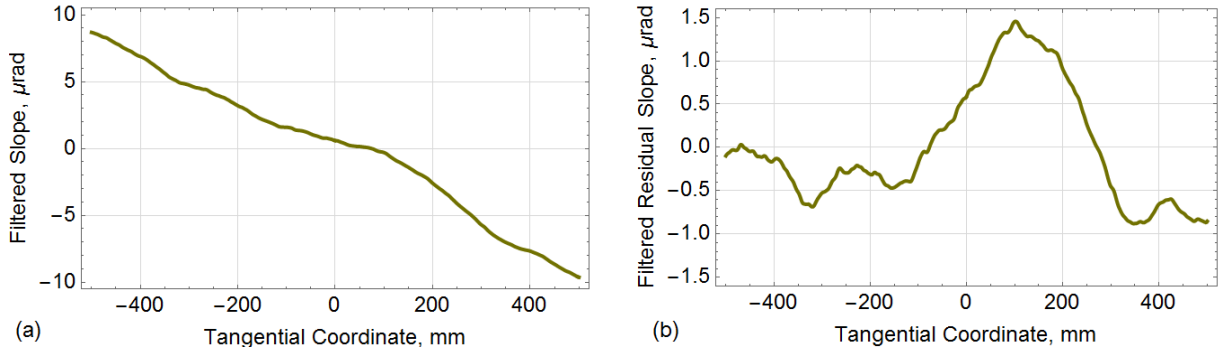


Figure 9: (a) The carriage pitch angle variation as measured in the carriage reference channel with the AC-2 (in the AC *X*-angular channel) and the reference mirror on the carriage platform (Fig. 1). (b) The residual nonlinear pitch error of the carriage translation after subtraction from the trace in plot (a) the best fit linear variation corresponding to the cylindrical shape of the granite beam appeared due to the fabrication imperfection and gravity sag. The detrended cylindrical shape corresponds to the radius of curvature of 56.9 km.

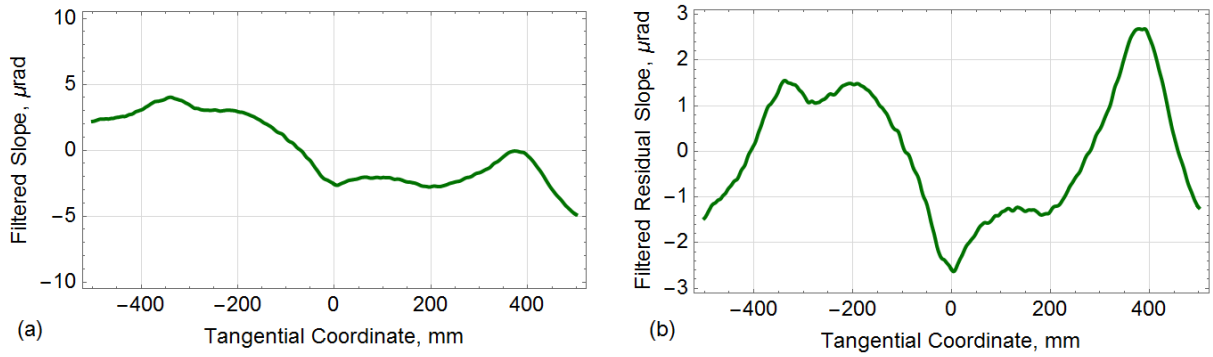


Figure 10: (a) The carriage yaw angle variation as measured in the carriage reference channel with the AC-2 (in the AC *Y*-angular channel) and the reference mirror on the carriage platform (Fig. 1). (b) The residual nonlinear yaw error of the carriage translation after subtraction the trace in plot (a) the best fit linear variation corresponding to the cylindrical shape of the granite beam due to the fabrication imperfection. The detrended cylindrical shape corresponds to the radius of curvature of ~ 136.9 km.

The variation of the carriage yaw angle (Fig. 10) is not affected (in the first order approximation) by gravity; and the PV wiggling error is less than 10 µrad. However, most of the variation still corresponds to the cylindrical shape (linear slope variation) that is probably due to the fabrication imperfection of the granite beam. The nonlinear residual slope variation is about 5 µrad (PV).

The repeatability of the carriage translation was tested via comparison of two sequential measurements in the carriage reference channel. Figure 11 shows the untreated difference of the carriage wobbling and wiggling effects in the repeated measurements.

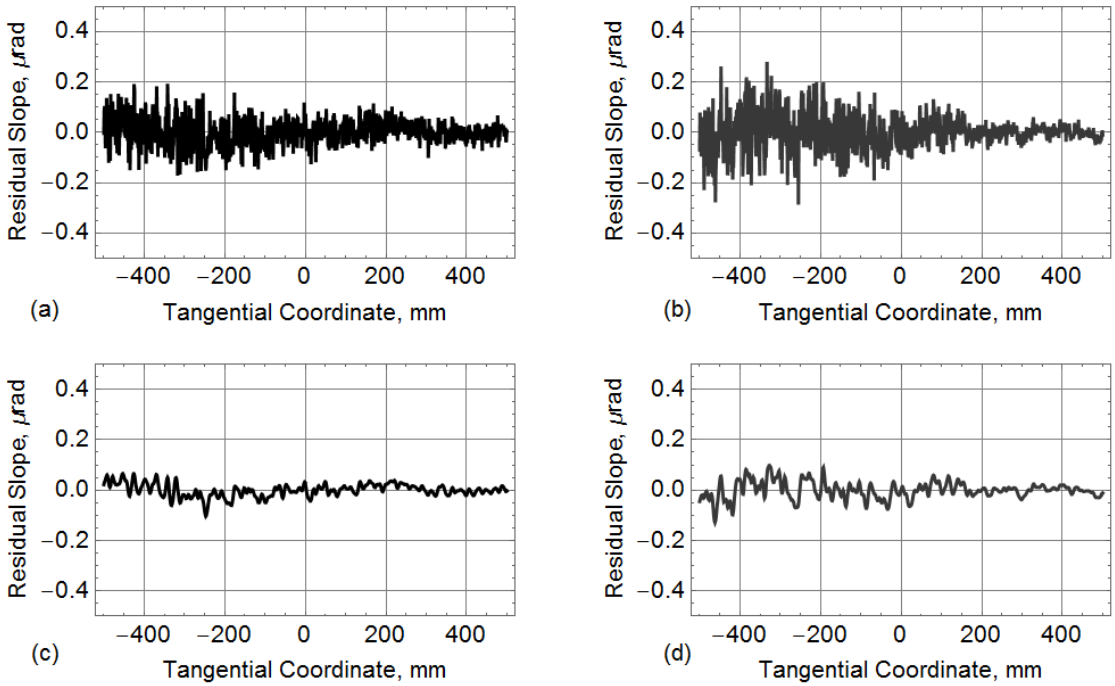


Figure 11: Test of the carriage translation repeatability, (a) difference of the pitch angle variations recorded in the AC *X*-angular channel and (b) difference of the yaw angle variations recorded in the AC *Y*-angular channel measured in two repeated runs of 8 optimally arranged scans. (c) and (d) The same traces as in (a) and (b) but filtered as discussed in Sec. 6.1. The rms variations of the pictures (a) through (d) are 54.7 nrad, 68.9 nrad, 25.3 nrad, and 33.9 nrad, respectively; otherwise stated, the filtering reduces the rms by a factor of two for both the pitch and yaw angular variations.

The data in Fig. 11 was not filtered and the corresponding differences are strongly affected by the air convection noise. The magnitude of the air convection error is increasing with increase of the optical path in the course of the carriage translation. After filtering, there is still a quasi-periodic residual oscillation. The oscillation has the same origin as the ones with 5.2 mm period observed in the filtered residual pitch slope trace of the slab measured without shielding (see Sec. 6.1 and Fig. 8a) and appeared due to the air convection induced by the cycling operation of the lab air conditioner.

### 6.3 Angular errors of the slab translation

The wobbling and wiggling effects of the slab translation are illustrated in Figs. 12 and 13 as measured in the slab reference channel with the AC-4 and the slab reference mirror (Fig. 1). The corresponding traces are the result of averaging of 8 optimally arranged scans[39] used to suppress the measurement random and drift errors (see Sec. 2).

The PV variation of the slab pitch angle when scanning over ±150 mm (Fig. 12a) is about 8 µrad. Most of the variation corresponds to the cylindrical shape (linear slope variation) that is probably due to the fabrication imperfection of the OSMS gantry base and, possibly, a gravity sag. The nonlinear residual slop variation is about 0.3 µrad (PV) and 57 nrad (rms). Note that around the central part of the scanning range between -25 mm and -70 mm, the wobbling error is almost perfectly linear, corresponding to the radius of curvature of ~37.2 km. This scanning range is preferable in 2D slope metrology with relatively short scanning in the sagittal direction.

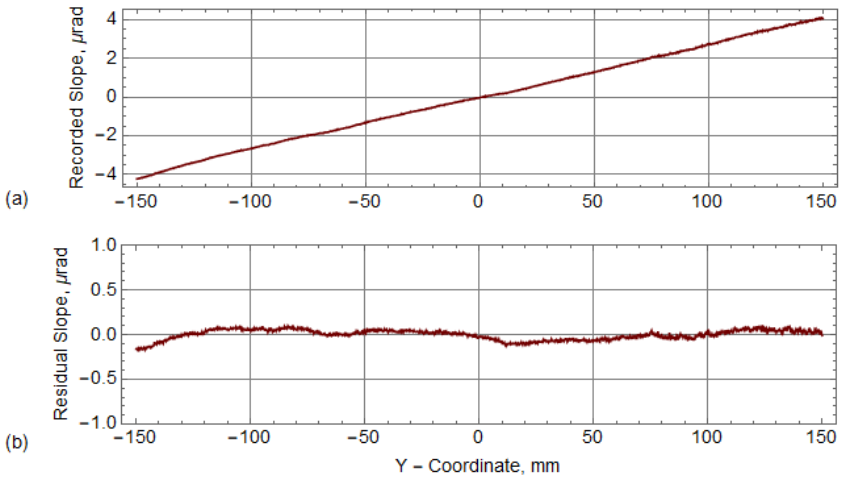


Figure 12: (a) The slab pitch angle variation as recorded in the AC-4 *Y*-angular channel using the slab reference channel mirror (Fig. 1). (b) The residual nonlinear pitch error of the slab translation after subtraction from the trace in plot (a) of the best fit linear variation corresponding to the cylindrical shape of the gantry base. The detrended cylindrical shape corresponds to the radius of curvature of 36.9 km. The residual slope variation is 57 nrad (rms).

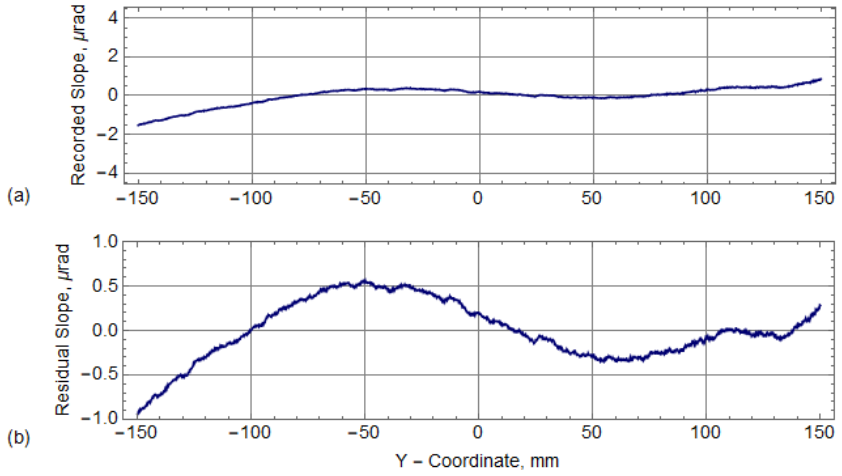


Figure 13: (a) The slab yaw angle variation as recorded in the AC-4 *X*-angular channel using the slab reference channel mirror (Fig. 1). (b) The residual nonlinear yaw error of the slab translation after subtraction from the trace in plot (a) of the best fit linear variation. The detrended cylindrical shape corresponds to the radius of curvature of 257.6 km. The residual slope variation is about 0.34 μrad (rms) and ~1.5 μrad (PV).

The variation of the slab yaw angle (Fig. 13) is not affected (in the first order approximation) by the gravity; and the PV wiggling error is only about 2.5 μrad. However, the most of the variation still corresponds to the cylindrical shape (linear slope variation) that is probably due to the fabrication imperfection of the granite. The nonlinear residual slop variation is also smaller, of about 1.5 μrad (PV) and 0.34 μrad (rms).

The additional measurements with shielded optical path (similar to the ones in Figs. 12 and 13) have shown that the repeatability of the slab wobbling and wiggling errors is approximately 20 nrad (rms).

In spite of the observed high repeatability of the slab wobbling and wiggling errors, the errors can generally depend on the environmental conditions (for example, humidity and temperature) and experimental arrangement (for example, different loading). Therefore, the monitoring of the errors in the course of measurements with the dedicated reference channel is important for high accuracy 2D surface slope metrology.

# 7. ANGULAR ERRORS OF THE TTPR STAGE

In this section, we discuss the results of the tests with the TTPR stage carried out to understand the performance of the stage in two most important applications. First, the accuracy and repeatability of the automatic flipping of a SUT used in the course of a measurement run arranged according to the advanced optimal scanning strategies[33] (see also Sec.2). Second, we investigated the ability of the stage to pitch-tilt of a SUT with the resolution required for calibration of the profiler with the face-up oriented SUT as a reference mirror (see discussion in Sec. 3.4).

### 7.1 Accuracy of 180-degree flipping of a SUT with the TTPR stage

According to the consideration in Sec. 4, the accuracy required for 180-degree rotation (flipping) of a sagittaly curved mirror with the extreme parameters of the sagittal radius of curvature of 30 mm and the length of 600 mm, is < 30 μrad.

The stage 180-degree flipping performance was tested with the AC-3 (Fig. 1) and a reference cube placed with a kinematic mount on the TTPR stage platform in the center of the stage rotation. The cube has five high quality mirror-like reference surfaces. Using the AC-1, the top reference surface of the cube was precisely aligned to be orthogonal to the rotation axis. After that, with the AC-3 we measured the error of the orientation of the two opposite reference surfaces of the cube appeared upon 180-degree rotation. In order to exclude the fabrication error of the cube, the measurement was repeated with the cube manually rotated by 180 degrees and averaged with the first one. The measurements were cycled eight times each to check the repeatability of the rotation. The accuracy of the 180-degree rotation determined this way is within ±1 μrad of uncertainty (largely attributed to air convection noise), well below the requirement.

The results of the rotation tests suggest for the performance of the rotation that is adequate for using the stage for the calibration of the profilometer with a side-facing SUT as a reference mirror.

### 7.2 Performance of the TTPR stage to pitch angle tilting

The performance of the TTPR stage to the pitch angle tilting was tested with the stage rotation orientation adjusted to provide the pitch tilting by changing the position of only one *Z*-axis translation motor (see Sec. 5.3). The pitch angle of a reference flat mirror placed to the stage platform was recorded in the AC-1 *X*-angular channel. In order to decrease the lateral and vertical displacement of the mirror while tilting, it was located just above the tilt rotation axis determined with the positions of the two stationary *Z*-axis translation motors.

Figure 14 depicts the pitch angle as a function of the *Z*-position of the driving motor.

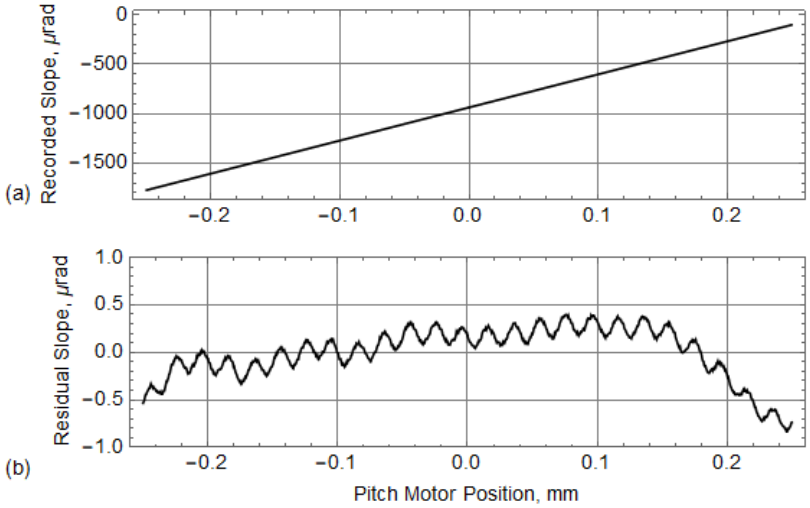


Figure 14: (a) The pitch angle dependence on the *Z*-position of the driving motor as recorded in the AC-1 *X*-angular channel. The flat reference mirror is located above the tilt rotation axis determined with the positions of the two stationary *Z*-axis translation motors. The Z-translation was in the upward direction. (b) The residual pitch angle variation after subtraction from the trace in plot (a) of the best fit linear dependence. The PV variation of the pitch error is about 1.5 μrad.

In Fig. 14a, the pitch driving motor was scanning over 500 μm with 0.5 μm increment. With an approximately 300 mm lever to the fulcrum of the pitch adjustment, this corresponds to a total ideal angle change of 1666.7 μrad. The range is a

compromise between the whole dynamic range of the AC of ~9.2 mrad and the desired high resolution of the *Z*-axis translation increment.

The non-linear residual error of the pitch angle (Fig. 14b) has a strong periodicity of ~20 μm with the amplitude of about ±0.15 μrad. The period corresponds to the angular oscillations with period of ~65 μrad. In order to understand the origin of the oscillation (due to the AC or the stage), we carried out two additional measurements similar to the one in Fig. 14 but performed with the AC pitch alignments differed by approximately 30 μrad. After the AC realignment, the phase of the oscillations was unchanged. This suggests that the oscillations are due to the motor motion. Where the pitch motors are not active during the course of data acquisition, and only tilt the stage between scans within a measurement run, this will not impact measurement results.

Figure 15 illustrates the repeatability of the pitch angle tilting with TTPR stage. It shows a difference of the trace in Fig. 14 and a measurement repeated at the same experimental arrangement. The repeatability is characterized with the PV and rms variations of 0.43 μrad and 86 nrad, respectively.

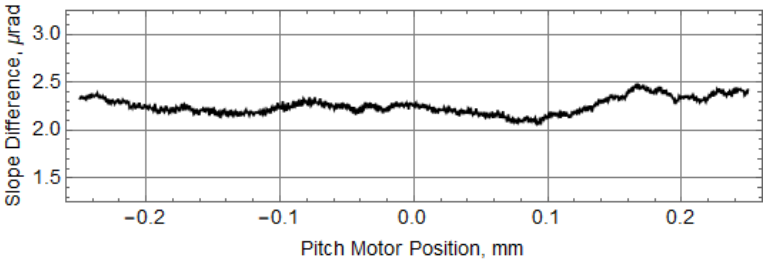


Figure 15: The difference of two sequential measurements (one is depicted in Fig. 14) of the pitch angle dependence on the *Z*-position of the driving motor. The PV variation of the difference angle trace is 0.43 μrad.

From the level of the random noise in the data in Fig. 15, we estimate the resolution of the pitch angle tilting to be better than ±20 nrad. The resolution determines the expected accuracy of the pitch angle tilting with TTPR stage when the AC measurements are used in the feedback of the tilt. This is adequate to the usage of the stage for the self-calibration with the face-up oriented SUT as a reference mirror. The implementation of the AC measurements to control the pitch tilt with the OSMS data acquisition and motion control software is in progress.

## 8. CONCLUSION

In this article, we have presented the results of comprehensive characterization of the multifunctional translation system of a new Optical Surface Measuring System under development at the ALS XROL. The OSMS MFTS system comprises a 2D-translation granite gantry system and a high precision tilting and flipping stage. The performed investigations have confirmed that the performance of the MFTS is adequate to the needs for super high accuracy 2D slope profilometry with state-of-the-art x-ray optics.

We have investigated the capability of the OSMS equipped with a set of four electronic autocollimators to measure the SUTs in different orientation, face-up and side-facing. The additional reference channels provide a high accuracy monitoring of the wobbling and wiggling of the carriage and slab translations in the tangential (*X*) and sagittal (*Y*) directions.

We have demonstrated that the problem of air-convection noise in the *X*-reference channel can be effectively solved with an appropriately selected filtering of the reference slope data.

The tests performed with the TTPR stage have confirmed a high (on the level of ~1 μrad) accuracy of the automatic flipping of a SUT. This is much better than the accuracy required for flipping of a SUT in a measurement run arranged according to the advanced optimal scanning strategies.[33] Moreover, the high repeatability of the rotation provides a possibility for using the stage for the self-calibration of the OSMS slope profiler with a side-facing SUT as a reference mirror.

We have also investigated and demonstrated the ability of the stage to pitch-tilt of a SUT with the resolution required for the self-calibration with the face-up oriented SUT as a reference mirror. Implementation of this self-calibration method is in progress. When realized, the self-calibration will allow us to solve the problem of the absolute AC calibration that relates to the strong dependence of the calibration on the peculiarities of the measurement set-up and the SUT.

The performed investigations allow us to estimate the ultimate accuracy of a single run of a 2D measurement with the OSMS in the considered set-up configuration and with using the suggested methods and techniques for suppression of the measurement errors to be better than 50 nrad.

## ACKNOWLEDGEMENTS

We are thankful to Chris Hernikl and Davide Bianculli for the help with the OSMS set-up. J. A. and T. N. are very grateful to the ALS for providing the opportunity to work in a top level scientific environment and especially to his supervisor V. V. Y. for welcoming them to the ALS, and to ENSICAEN for giving him the opportunity for the internship. The Advanced Light Source is supported by the Director, Office of Science, Office of Basic Energy Sciences, Material Science Division, of the U.S. Department of Energy under Contract No. DE-AC02- 05CH11231 at Lawrence Berkeley National Laboratory.



## REFERENCES

[1] ALS-U, https://als.lbl.gov/als-u/.
[2] Kevan, S., Chair, [ALS-U: Solving Scientific Challenges with Coherent Soft X-Rays], Workshop report on early science enabled by the Advanced Light Source Upgrade, ALS, LBNL, Berkeley, CA, (2017) https://als.lbl.gov/wp-content/uploads/2017/08/ALS-U-Early-Science-Workshop-Report-Full.pdf.
[3] Samoylova, L., Sinn, H., Siewert, F., Mimura, H., Yamauchi, K., and Tschentscher, T., "Requirements on Hard X-ray Grazing Incidence Optics for European XFEL: Analysis and Simulation of Wavefront Transformations," Proc. SPIE 7360, 73600E/1-9 (2009).
[4] Assoufid, L., and Rabedeau, T., Co-Chairs, "X-ray Mirrors," in: X-ray Optics for BES Light Source Facilities, Report of the Basic Energy Sciences Workshop on X-ray Optics for BES Light Source Facilities, D. Mills and H. Padmore, Co-Chairs, pp. 118-129, U.S. Department of Energy, Office of Science, Potomac, MD, (2013); http://science.energy.gov/~/media/bes/pdf/reports/files/BES_XRay_Optics_rpt.pdf.
[5] Yashchuk, V. V., Samoylova, L., and Kozhevnikov, I. V., "Specification of x-ray mirrors in terms of system performance: A new twist to an old plot," Proc. SPIE 9209, 92090F/1-19 (2014).
[6] Yashchuk, V. V., Samoylova, L., and Kozhevnikov, I. V., "Specification of x-ray mirrors in terms of system performance: A new twist to an old plot," Opt. Eng. 54(2), 025108/1-13 (2015).
[7] Cocco, D., "Recent Developments in UV Optics for Ultra-Short, Ultra-Intense Coherent Light Sources," Photonics 2015, 2(1), 40-49 (2015).
[8] Idir, M., and Yashchuk, V. V., Co-Chairs, "Optical and X-ray metrology," in: X-ray Optics for BES Light Source Facilities, Report of the Basic Energy Sciences Workshop on X-ray Optics for BES Light Source Facilities, D. Mills and H. Padmore, Co-Chairs, pp. 44-55, U.S. Department of Energy, Office of Science, Potomac, MD (2013); http://science.energy.gov/~/media/bes/pdf/reports/files/BES_XRay_Optics_rpt.pdf.
[9] Yashchuk, V. V., Artemiev, N. A., Lacey, I., McKinney, W. R. and Padmore, H. A., "Advanced environmental control as a key component in the development of ultra-high accuracy ex situ metrology for x-ray optics," Opt. Eng. 54(10), 104104/1-14 (2015); doi: 10.1117/1.OE.54.10.104104.
[10] Yashchuk, V. V., Artemiev, N. A., Lacey, I., McKinney, W. R. and Padmore, H. A., "A new X-ray optics laboratory (XROL) at the ALS: Mission, arrangement, metrology capabilities, performance, and future plans," Proc. SPIE 9206, 92060I/1-19 (2014); doi:10.1117/12.2062042.
[11] Kirschman, J. L., Domning, E. E., McKinney, W. R., Morrison, G. Y., Smith, B. V., Yashchuk, V. V., "Performance of the upgraded LTP-II at the ALS optical metrology laboratory," Proc. SPIE 0770A-1 (2008).

[12] McKinney, W. R., Anders, M., Barber, S. K., Domning, E. E., Lou, Y., Morrison, G. Y., Salmassi, F., Smith, B. V., Yashchuk, V. V., "Studies in optimal configuration of the LTP", Proc. SPIE 7801, 780106-11 (2010).
[13] Yashchuk, V. V., Barber, S., Domning, E. E., Kirschman, J. L., Morrison, G. Y., Smith, B. V., Siewert, F., Zeschke, T., Geckeler, R., Just, A., "Sub-microradian surface slope metrology with the ALS developmental long trace profiler," Nucl. Instr. and Meth. A 616, 212-223 (2010).
[14] Lacey, I., Artemiev, N. A., Domning, E. E., McKinney, W. R., Morrison, G. Y., Morton, S. A., Smith, B. V., and Yashchuk, V. V., "The developmental long trace profiler (DLTP) optimized for metrology of side-facing optics at the ALS," Proc. SPIE 9206, 920603/1-11, (2014); doi:10.1117/12.2061969.
[15] Goldberg, K. A., Yashchuk, V. V., Artemiev, N. A., Celestre, R, Chao, W., Gullikson, E. M., Lacey, I., McKinney, W. R., Merthe, D., and Padmore, H. A., "Metrology for the Advancement of X-ray Optics at the ALS," Synchrotron Radiation News 26(5), 4-12, (2013); http://dx.doi.org/10.1080/08940886.2013.832583.
[16] Yamauchi, K., Mimura, H., Inagaki, K., and Mori, Y., "Figuring with subnanometer-level accuracy by numerically controlled elastic emission machining," Rev. Sci. Instrum. 73(11), 4028-4033 (2002); doi: 10.1063/1.1510573.
[17] Yamauchi, K., Mimura, H., Inagaki, K., and Mori, Y., "Microstitching interferometry for x-ray reflective optics," Rev. Sci. Instrum. 74(5), 2894-2898 (2003); doi: 10.1063/1.1569405.
[18] Ohashi, H., Tsumura, T., Okada, H., Mimura, H., Masunaga, T., Senba, Y. Goto, S., Yamauchi, K., Ishikawa, T., "Microstitching interferometer and relative angle determinable stitching interferometer for half-meter-long X-ray mirror," Proc. SPIE 6704, 670405 (2007); doi: 10.1117/12.733476.
[19] Mimura, H., Yamamura, K,, Sano, Y., Ueno, K., Endo, K., Mori, Y., Yabashi, M,, Tamasaku, K., Nishino, Y., Ishikawa, T., and Yamauchi, K., "Relative angle determinable stitching interferometry for hard x-ray reflective optics," Rev. Sci. Instrum. 76(4), 045102 (2005); doi: 10.1063/1.1868472.
[20] Kimura, T., Ohashi, H., Mimura, H., Yamakawa, D., Yumoto, H., Matsuyama, S., Tsumura, T., Okada, H., Masunaga, T., Senba, Y., Goto, S., Ishikawa, T., and Yamauchi, K., "A stitching figure profiler of large x-ray mirrors using RADSI for subaperture data acquisition," Nucl. Instrum. and Meth. A 616 (2-3), 229-2232 (2010) [doi: 10.1016/j.nima.2009.11.014].
[21] Siewert, F., Noll, T., Schlegel, T., Zeschke, T. and Lammert, H. "The nanometer optical component measuring machine: a new sub-nm topography measuring device for X-ray optics at BESSY", in: AIP Conference Proceedings, vol. 705, American Institute of Physics, Mellville, NY, 2004, pp. 847–850.
[22] Siewert, F., Buchheim, J., Zeschke, T., Störmer, M., Falkenberg, G., and Sankari, R., "On the characterization of ultra-precise X-ray optical components: advances and challenges in ex situ metrology," J. Synchrotron Rad. 21, 968–975 (2014); doi:10.1107/S1600577514016221.
[23] Nicolas, J., Pedriera, P., Sics, I., Ramirez, C., and Campos, J., "Nanometer accuracy with continuous scans at the ALBA-NOM," Proc. SPIE 9962, Advances in Metrology for X-Ray and EUV Optics VI, 996203 (2016); doi:10.1117/12.2238128.
[24] Polack, F., Thomasset, M., Brochet, S., Rommeveaux, A., "An LTP stitching procedure with compensation of instrument errors: Comparison of SOLEIL and ESRF results on strongly curved mirrors," Nucl. Instrum and Methods A 616(2-3), 207-211 (2010);http://doi.org/10.1016/j.nima.2009.10.166.
[25] Siewert, F., Buchheim, J., and Zeschke, T., "Characterization and calibration of 2nd generation slope measuring profiler," Nucl. Instrum. Methods A 616(2-3), 119–127 (2010); http://doi.org/10.1016/j.nima.2009.12.033.
[26] Idir, M., Kaznatcheev, K., Dovillaire, G., Legrand, J., and Rungsawang, R., "A 2 D high accuracy slope measuring system based on a Stitching Shack Hartmann Optical Head," Opt. Exp. 22(3), 2770-2781 (2014); doi: 10.1364/OE.22.002770.
[27] Q-Sys, SHARPeR Eurostars project 8304; http://www.q-sys.eu/SHARPeR%20V2-0.pdf.
[28] Gubarev, M. V., Merthe, D. J., Kilaru, K., Kester, T., Ramsey, B., McKinney, W. R., Takacs, P. Z., Dahir, A., and Yashchuk, V. V., "Status of multi-beam long trace-profiler development," Proc. SPIE 8848, 88480L-1-7 (2013);doi: 10.1117/12.2027146.
[29] Cocco, D., Sostero, G., and Zangrando, M., "Technique for measuring the groove density of diffraction gratings using the long trace profiler," Rev. Sci. Instrum. 74(7), 3544-3548 (2003).
[30] Cocco, D., and Thomasset, M., "Measurement of groove density of diffraction gratings," in: Modern Developments in X-Ray and Neutron Optics, A. Erko, M. Idir, T. Krist, and A. G. Michette, Eds., Springer, New York (2008), pp. 207-211.
[31] Sheung, J., Qian, J., Sullivan, J., Thomasset, M., Manton, J., Bean, S., Takacs, P., Dvorak, J., and Assoufid, L., "Metrology of variable-line-spacing x-ray gratings using the APS Long Trace Profiler," Proc. SPIE 10385, 1038508 (2017); https://doi.org/10.1117/12.2279053.

[32] Lacey, I., Adam, J., Centers, G., Gevorkyan, G. S., Nikitin, S. M., Smith, B. V., and Yashchuk, V. V., "Development of a high performance surface slope measuring system for two-dimensional mapping of x-ray optics," Proc. SPIE 10385, 10385 – 16/1-13(2017).
[33] Yashchuk, V. V., Centers, G., Gevorkyan, G. S., Lacey, I., and Smith, B. V., "Correlation methods in optical metrology with state-of-the-art x-ray mirrors," Proc. SPIE 10612, Thirteenth International Conference on Correlation Optics, 106120O/1-23 (2018); doi: 10.1117/12.2305441.
[34] Yashchuk, V. V., Takacs, P. Z., McKinney, W. R., Assoufid, L., Siewert, F., Zeschke, T., "Development of a new generation of optical slope measuring profiler," Nucl. Instr. and Meth. A 649(1), 153-155 (2011) - LBNL-3975E; http://doi.org/10.1016/j.nima.2010.10.063.
[35] Assoufid, L., Brown, N., Crews, D., Sullivan, J., Erdmann, M., Qian, J., Jemian, P., Yashchuk, V. V., Takacs, P.Z., Artemiev, N. A., Merthe, D. J., McKinney, W. R., Siewert, F., Zeschke, T., "Development of a high-performance gantry system for a new generation of optical slope measuring profilers," Nucl. Instr. and Meth. A 710, 31-36 (2013); http://dx.doi.org/10.1016/j.nima.2012.11.063.
[36] Qian, J., Sullivan, J., Erdmann, M., Khounsary, A., and Assoufid, L., "Performance of the APS optical slope measuring system," Nucl. Instrum. and Meth. A 710, 48–51 (2013); https://doi.org/10.1016/j.nima.2012.10.102.
[37] Alcock, S. G., Sawhney, K. J. S., Scott, S., Pedersen, U., Walton, R., Siewert, F., Zeschke, T., Senf, F., Noll T., and Lammert, H., "The Diamond-NOM: A non-contact profiler capable of characterizing optical figure error with sub-nanometre repeatability," Nucl. Inst. and Methods A 616(2-3), 224-228 (2010).
[38] Y. Senba, H. Kishimoto, H. Ohashi, H. Yumoto, T. Zeschke, F. Siewert, S. Goto, T. Ishikawa, "Upgrade of long trace profiler for characterization of high-precision X-ray mirrors at SPring-8,"Nucl. Inst. and Meth. A 616 (2-3), 237-240 (2010).
[39] Yashchuk, V. V., "Optimal Measurement Strategies for Effective Suppression of Drift Errors," Rev. Sci. Instrum. 80, 115101-1-10 (2009); http://dx.doi.org/10.1063/1.3249559.
[40] Yashchuk, V. V., Artemiev, N. A., Lacey, I., and Merthe, D. J., "Correlation analysis of surface slope metrology measurements of high quality x-ray optics," Proc. SPIE 8848, 88480I-1-15 (2013); doi: 10.1117/12.2024694.
[41] Yashchuk, V. V., Irick, S. C., MacDowell, A. A., McKinney, W. R., Takacs, P. Z., "Air convection noise of pencil-beam interferometer for long-trace profiler," Proc. SPIE 6317, 63170D/1-12 (2006); https://doi.org/10.1117/12.681297.
[42] Yashchuk, V. V., McKinney, W. R., Warwick, T. Noll, T. Siewert, F., Zeschke, T., Geckeler, R. D., "Proposal for a Universal Test Mirror for Characterization of Slope Measuring Instruments," Proc. SPIE 6704, 67040A/1-12 (2007); doi:10.1117/12.732719.
[43] Yashchuk, V. V., Artemiev, N. A., Centers, G. P., Chaubard, A., Geckeler, R. D., Lacey, I., Marth, H., McKinney, W. R., Noll, T., Siewert, F., Winter, M., and Zeschke, T., "High precision tilt stage as a key element to universal test mirror for characterization and calibration of slope measuring instruments," Rev. Sci. Instrum. 87(5), 051904 (2016); doi: 10.1063/1.4950729.
[44] Geckeler, R. D., Artemiev, N. A., Barber, S. K., Just, A., Lacey, I., Kranz, O., Smith, B. V., and Yashchuk, V. V., "Aperture alignment in autocollimator-based deflectometric profilometers," Rev. Sci. Instrum. 87(5), 051906/1-8 (2016); doi: 10.1063/1.4950734.
[45] Ali, Z., Artemiev, N. A., Cummings, C. L., Domning, E. E., Kelez, N., McKinney, W. R., Merthe, D. J., Morrison, G. Y., Smith, B. V., and Yashchuk, V. V. "Automated suppression of errors in LTP-II slope measurements with x-ray optics," Proc. SPIE 8141, 81410O-1-15 (2011); http://dx.doi.org/10.1117/12.894061.
[46] Qian, S., and Idir, M., "Innovative nano-accuracy surface profiler for sub-50 nrad rms mirror test," Proc. SPIE 9687, 96870D/1-10 (2016); doi:10.1117/12.2247575.
[47] Q-Sys Company website; http://www.q-sys.eu/the_company.html.
[48] Barber, S. K., Morrison, G. Y., Yashchuk, V. V., Gubarev, M. V., Geckeler, R. D., Buchheim, J., Siewert, F., Zeschke, T., "Developmental long trace profiler using optimally aligned mirror based pentaprism," Opt. Eng. 50(5), 053601-1-10 (2011); https://doi.org/10.1117/1.3572113.
[49] Barber, S. K., Geckeler, R. D., Yashchuk, V. V., Gubarev, M. V., Buchheim, J., Siewert, F., Zeschke, T., "Optimal alignment of mirror based pentaprism for scanning deflectometric devices," Opt. Eng. 50(7), 0073602-1-8 (2011); https://doi.org/10.1117/1.3598325.
[50] Just, A., Krause, M., Probst, R., and Wittekopf, R., "Calibration of high-resolution electronic autocollimators against an angle comparator," Metrologia 40, 288-294 (2003).
[51] Geckeler, R. D., and Just, A., "Optimized use and calibration of autocollimators in deflectometry," Proc. SPIE 6704, 670407/1-12 (2007).

[52] Geckeler, R. D., and Just, A., "Distance dependent influences on angle metrology with autocollimators in deflectometry," Proc. SPIE 7077, 70770B/1-12 (2008).
[53] Geckeler, R., Just, A., Krause, M., Yashchuk, V. V., "Autocollimators for Deflectometry: Current Status and Future Progress," Nucl. Instr. and Meth. A 616, 140-146 (2010).
[54] Moeller Wedel Optical GmbH, "Electronic Autocollimators;" https://www.haag-streit.com/fileadmin/Moeller_wedel_optical/Brochures/Electronic_Autocollimators/ELCOMAT__English.pdf.
[55] Yashchuk, V. V., "Sub-microradian Surface Slope Metrology at the ALS Optical Metrology Laboratory and around the World," Oral presentation at the First Meeting on Development of a New Optical Surface Slope Measuring System - OSMS-I (ALS, Berkeley, March 26, 2010).
[56] Schindler, A., Haensel, T., Nickel, A., Thomas, H.-J., Lammert, H., Siewert, F., "Finishing procedure for high performance synchrotron Optics," Proc. SPIE 5180 (1), 70-78 (2004).
[57] Probst, R., Wittekopf, R., Krause, M., Dangschat, H., and Ernst, A., "The new PTB angle comparator," Meas. Sci. Technol. 9, 1059 – 1066 (1998).
[58] Just, A., Krause, M. Probst, R., Bosse, H., Haunerdinger, H., Spaeth, C., Metz, G., and Israel, W., "Comparison of angle standards with the aid of a high-resolution angle encoder," Precis. Eng. 33(4), 530-3 (2009).
[59] Geckeler, R. D., Link, A., Krause, M., and Elster, C., "Capabilities and limitations of the self-calibration of angle encoders," Meas. Sci. Technol. 25, 055003/1-10 (2014).
[60] Lacey, I., Geckeler, R. D., Just, A., Siewert, F., Arnold, T., Paetzelt, H., Smith, B. V., and Yashchuk, V. V., "Optimization of size and shape of aperture in autocollimator-based deflectometric profilometers," Abstract of the oral presentation at the 6th International Workshop on X-ray Optics and Metrology, The SRI2018 Satellite Workshop (IWXM 2018) (Hsinchu, Taiwan, June 6-9, 2018); http://iwxm2018.nsrrc.org.tw/site/page.aspx?pid=23&sid=1203&lang=en.
[61] Siewert, F., Buchheim, J., Höft, T., Zeschke, T., Schindler, A., Arnold, T., "Investigations on the spatial resolution of autocollimator – based slope measuring profilers," Nucl. Instrum. Methods Phys. Res. A 710 42–47 (2013).
[62] Siewert, F., Zeschke, T., Arnold, T., Paetzold, H., and Yashchuk, V. V., "Linear chirped slope profile for spatial calibration in slope measuring deflectometry," Rev. Sci. Instrum. 87(5), 051907/1-8 (2016); doi: 10.1063/1.4950737.
[63] OPTODYNE, Inc, [Model LDS-1000 Laser Doppler scale]; http://www.optodyne.com/opnew5/products/lds1000.pdf.
[64] Attocube, Inc., [IDS3010 integrated displacement sensing]; http://www.attocube.com/attosensorics/ids-sensors/ids3010/.